

Void and pore formation inside the hair cortex by a denaturation and super-contraction process occurring during hair setting with hot irons

MANUEL GAMEZ-GARCIA, *BASF Care Chemicals*,
500 White Plains Rd, Tarrytown, NY 10591.

Synopsis

An analysis of hair fibers from donors that frequently use hot irons for hair straightening showed the presence of multiple pores and voids ($\phi \sim 0.1\text{--}1.5 \mu\text{m}$) that extend from the cuticle sheath to regions inside the hair cortex. Pore formation in the cortex was found to be confined at its periphery and could be reproduced in the laboratory with virgin hair fibers after the application of various hot-iron straightening cycles. The appearance of pores and voids in the cortex was found to be associated to the production of hot water vapor while the fiber is undergoing mechanical elongation or contraction. The number of pores was seen to rapidly increase with temperature in the range from 190 to 220°C and also with the number of straightening cycles. Larger hair voids ($\phi \sim 2\text{--}5 \mu\text{m}$) were also detected in the cortex. The small pores found at the cortex periphery appear to occur by the simultaneous occurrence of rearrangement of hair proteins, fiber mechanical contraction/expansion, and the flow of super-heated steam. Hot irons create, thus, the conditions for the onset of pore formation as the high temperatures produce superheated steam and soften the native state of hair proteins by a process involving denaturation and changes in the crystalline regions.

INTRODUCTION

Recently, the cosmetic community has shown a strong interest in understanding the damaging effects produced by hot irons in hair. Efforts directed to achieve this objective have already unveiled some of the various physical and chemical changes that take place in hair during its exposure to hot irons. For instance, it has been reported that the denaturation enthalpy of hair is significantly modified after its exposure to temperatures above 150°C (1–4). Chemical changes in the protein structure of the hair cortex have also been observed to occur as a consequence of the hot-iron high temperatures. Tryptophan degradation and the appearance of other oxidation products are among the main chemical changes reported by some authors (5–6). Cuticle cell lifting, cracking, and hair breakage were also shown to occur when hot irons were applied to hair under harsh conditions (7).

In this paper results are presented showing that micropores and voids are formed inside the hair cortex after hot-iron treatments. As it will be discussed in the Results section, micropores and voids may be formed both in the cuticle sheath and cortex as a consequence of the combined action of protein denaturation, protein chemical changes, and the explosive evaporation of water that takes place inside the hair cortex during hot-iron

applications. Interest on these pores arose from a microscopic investigation made on hair bundles obtained from donors who frequently use hot irons. The investigation revealed that a large number of fibers from these donors contained a high number of pores. Pores in hair have already been reported by various authors, although, the pores found by these researches does not seem related to hair treatment with hot irons (8–10). In the result section it will be shown that, pores and voids of various sizes, can actually be re-produced in the laboratory when hair is exposed to heat under various controlled conditions.

METHODOLOGY

The method used to detect the presence of pores in the hair fibers was by Microscopy using a Hi-Scope from Hirox Model KH-3000. The hair was of Brown European Wavy Virgin Hair from International Hair Importers ~ 8 inches long. Various treatment cycles of hot ironing were applied to hair tresses ~ 0.5 g in weight. The use of this amount of hair allowed the hair fibers to evenly spread when placed under the hot-iron jaws and ensured that most of them were in contact with the iron surface. Also, whenever needed, cycles of hot ironing were applied to single hair fibers with a mini-hot iron to confirm observations. Each treatment cycle of hot ironing consisted of the following steps: 1) 30 s shampooing with a clarifying shampoo, 2) 30 s rinsing with tap water, 3) Blot drying with a towel for 10 s, 4) Blow drying until the hair dried to ~ 80% of its moisture content, 5) Three hot-iron passes over the hair tresses from root to tip at temperatures ranging between 180 and 220°C depending on the requirements. Two hot-iron speeds were used during hot ironing, one considered a normal speed ~ 1.0 in/s and the other one considered a low speed ~ 0.2 in/s, and 6) After this process the hair tresses/fibers were left at rest at room temperature conditions for three hours before applying the next treatment cycle.

The method of pore detection consisted in shifting the plane of focus of the microscope from the hair surface into regions inside the cortex according to the diagram showed in Figure 1. This process allowed the visualization of pores and voids inside the cuticle sheath and cortex. The existence of pores was revealed by the contrast of light scattering patterns produced by a mismatch in the indexes of refraction between empty spaces of pores and cortex. Later, counting of the pore number and measurements of their size was made by image analysis using the software Pax-It from Midwest Information Systems.

RESULTS

DETECTION OF MICROPORES

In Figures 2a and 2b are shown micrographs of a hair fiber with five treatment cycles of hot-iron at 180°C showing typical micropores inside the hair cortex. Figure 2a displays the image of the hair surface taken without shift in plane of focus; this picture clearly shows the topology at the cuticle surface. In principle, by looking at this picture it could be inferred that there is no apparent physical change on the hair after its exposure to hot-iron treatment. However, in Figure 2b it can be seen that when the plane of focus of the

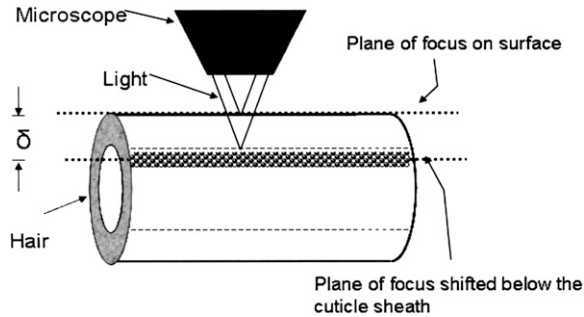


Figure 1. Diagrammatic representation of microscope and hair fiber showing focusing of microscope beam at the hair surface without shift in plane of focus, and at a distance (δ) deep inside into the hair fiber after the plane of focus was shifted.

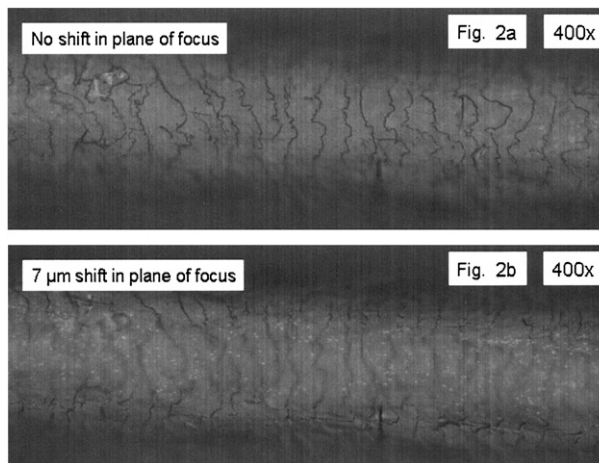


Figure 2. Micrograph of a hair fiber ($\phi \sim 78 \mu\text{m}$) taken without shift in plane of focus (2a), and after the plane of focus was shifted towards regions inside the cortex by $7 \mu\text{m}$ (2b). The hair fiber was subjected to three hot-iron treatments at 180°C with a hot-iron speed of 1 in/s.

microscope is shifted $\sim 7 \mu\text{m}$ towards the center of the hair fiber, a large number of white dots appears in the hair. These white dots are actually micropores localized inside the hair cortex close to its surface; they appear as white dots because the light scattering patterns produced by their empty spaces contrast with the translucency of the cortex.

Initially, it was thought that the presence of these pores arose as a consequence of hair chemical treatments such as bleaching or permanent waving. However, a systematic analysis of sets of 200 hair fibers that were bleached with various degrees of intensity failed to show the appearance of pores. Likewise, sets of hair fibers from bundles that were treated with permanent waving solutions also did not show the presence of such pores. Furthermore, microscopic analysis revealed that only hot-iron treatments were able to create pores in virgin hair fibers that didn't have any form of damage before treatment. It was difficult to measure with precision the size of the micropores; however, their apparent sizes as measured by image analysis indicates that their diameter ranges between 0.1 and 1.5 micrometers.

EFFECTS OF HOT-IRON TEMPERATURES LOWER THAN 180°C AND NORMAL SPEEDS.

Pore density or number of pores per unit area appeared to increase with the number of hot iron treatments at hot iron speeds of 1 in/s (see Figures 3a and 3b). Pores were also observed to form in hair that had no cuticle cells on its surface (see Figures 4a and 4b). For instance, Figure 4a shows a micrograph of a hair fiber with its surface devoid of cuticle cells. The image displays the bare surface of the cortex as this picture was taken with no shift in plane focus. In contrast, Figure 4b displays an image of the same fiber where multiple pores can be observed after the microscope plane of focus was shifted.

In order to obtain more information about the pores, various digital filters were applied to the picture files to separate pores from other features in the images. For instance, in Figures 5a and 5b it can be seen that by using image filtering the pores can be highlighted while the remainder of the image was transformed into dark background. Once the pores are clearly differentiated in the image it was possible to count them and to

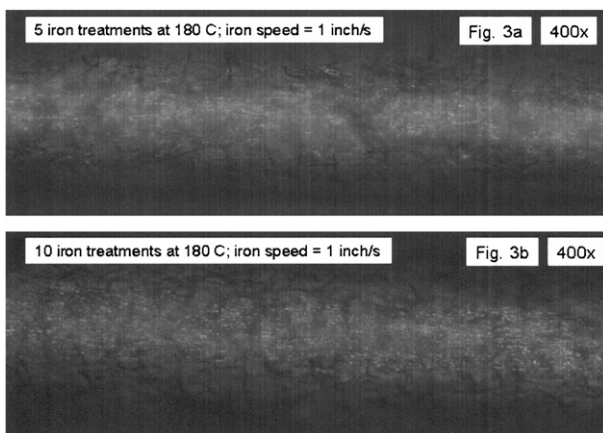


Figure 3. Micrographs of hair fibers ($\phi \sim 73 \mu\text{m}$) subjected to five (3a) and ten (3b) hot-iron treatments at 180°C using a hot-iron speed of ~ 1 in/s.

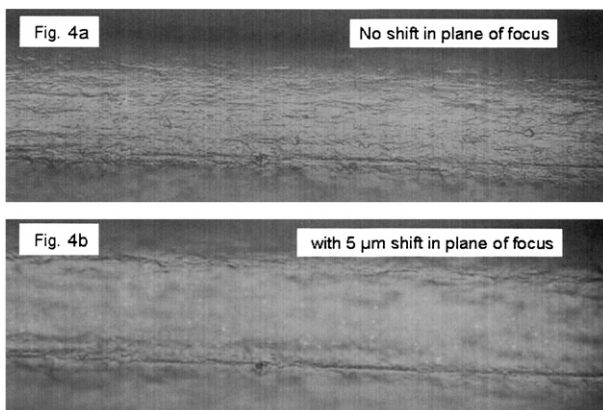


Figure 4. Micrographs (400 \times) of a hair fiber ($\phi \sim 68 \mu\text{m}$) devoid of cuticle cells before (4a), and after (4b) the plane of focus was shifted in $5 \mu\text{m}$. The fiber was subjected to five hot-iron treatments at 180°C using a hot-iron speed of ~ 1 in/s.

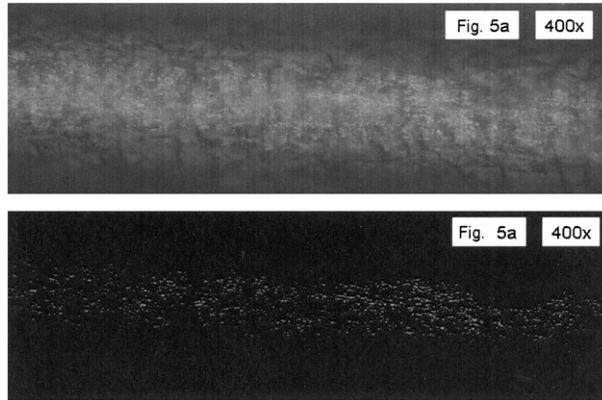


Figure 5. Micrograph of a hair fiber ($\phi \sim 76 \mu\text{m}$) subjected to five treatments of hot ironing showing the presence of pores at a depth of $10 \mu\text{m}$ inside the cortex (5a). The image in Figure 5a was then thresholded to create a binary image by using image analysis software in order to separated the pores from a black background (Figure 5b).

obtain a distribution profile of their size by area (see Figure 6). By using this counting technique in combination with the ability to shift the plane of focus it was soon found that micropore formation occurs mainly at the cortex periphery (see Figure 7). Further analysis based on this counting technique led to three groups of observations related to the mechanism of pore formation.

The first group of observations is related to the presence of moisture in the hair fiber and to changes in its dimensions. These observations revealed that a critical factor in the formation of pores is the combination of moisture and fiber changes in dimensions; if the fiber is not elongated or contracted pore formation is practically non-existent. For instance, in Figure 8 it can be seen that the number of pores as a function of hot-iron treatments, at normal speeds, is very low when the fibers are dried, either, with or without elongation. However, in the same figure it can be seen that when the fibers contain moisture the overall number of pores increases very rapidly; although, the increments are substantially higher when the fibers are wet and elongated. The term “elongation” refers here to fiber extension created by fiber dragging due to hot-iron friction. Pores were also

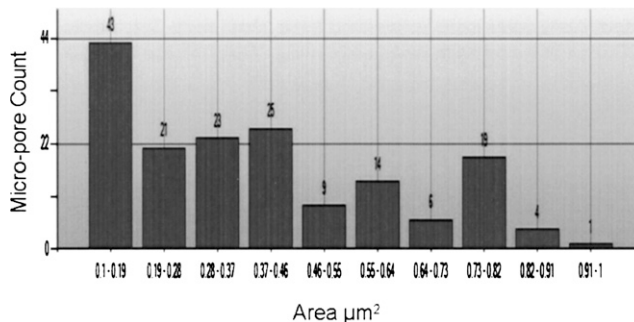


Figure 6. Micropore count and profile distribution by pore size obtained in a fiber area of 0.06 mm^2 by image analysis.

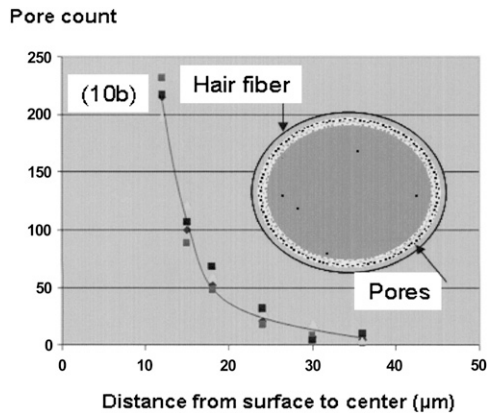


Figure 7. Pore count in an area of 0.06 mm^2 as a function of distance toward the center of the cortex for a set of four fibers of $\phi \sim 72 \text{ }\mu\text{m}$ subjected to ten hot-iron treatments at 180°C using a hot-iron speed of 1 in/s.

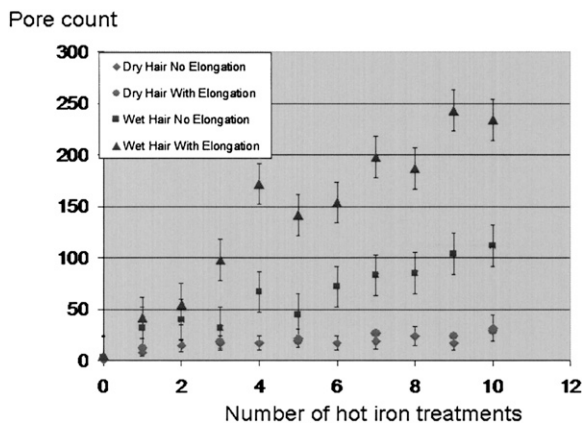


Figure 8. Graph showing total number of pores in an area of 0.06 mm^2 as a function of hot-iron treatments ($T \sim 180^\circ\text{C}$ and hot-iron speed $\sim 1 \text{ in/s}$) with moisture and elongation as parameters. The content of moisture in the hair fiber for the wet and dry conditions corresponded to equilibration at 82% and 10% RH, respectively. The fiber elongation produced after hot ironing was $\sim 4\%$.

formed when fibers containing moisture underwent longitudinal free contraction upon contact with a hot plate at temperatures ranging between 180 and 200°C .

The second group of observations is related to the effect of temperature as shown in Figure 9 where it can be seen that significant levels of pore formation start to occur around 150°C , after which the number of pores increase monotonically with temperature for a fixed number of hot-iron cycles. Finally, the third group of observations relates to the occurrence of fiber super-contraction. Namely, it was observed that hair fibers which were hot ironed, elongated, and with pores in their cortex underwent later super-contraction after they were wet and/or re-heated again. Also, hair fibers that were immersed in water/ethanol solutions showed high levels of pore formation after contacting hot surfaces ($180\text{--}200^\circ\text{C}$). Table I lists the degree of super-contraction associated to the various levels of elongation during hot ironing. Super-contraction and denaturation are common phenomena in keratin fibers and have been associated to the melting and disarray of ordered protein structures. These phenomena have been reported to occur as a consequence of

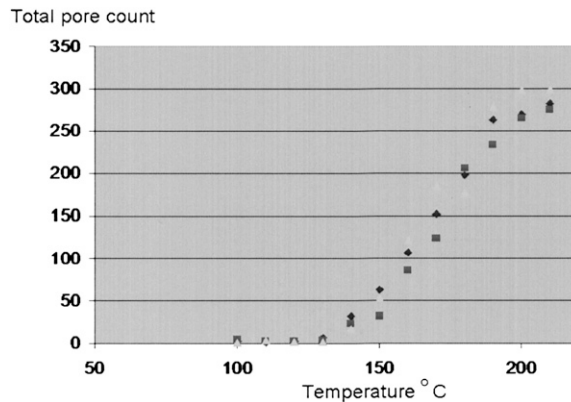


Figure 9. Graph showing total count of number of pores in an area of $\sim 0.06 \text{ mm}^2$ as a function of temperature while keeping the number of hot-iron treatments constant at five. The data represent counts of three fibers $\sim 68 \mu\text{m}$ in diameter.

fiber excessive elongation, its exposure to high temperatures, exposure to alcoholic solutions, and also after chemical changes that destabilize its structure, i.e. breakage of hydrogen and disulfide bonds (11–14).

According to the ongoing considerations it is straightforward that pore formation is associated to the following phenomena: 1) Protein denaturation involving chemical changes due to hydrogen and disulfide bond breakage, 2) Water evaporation, and 3) Fiber elongation and super-contraction. The fact that pores start to form at around $\sim 150^\circ\text{C}$, and that water and mechanical elongation/contraction are necessary for their creation, suggests that pore formation involves a process of protein denaturation. During this process a fraction of the hair crystalline structure will undergo a transition into a disordered structure. The denatured regions will be further disrupted by the explosive evaporation of water and by protein motion activated, either, by elongation or contraction creating, thus, the observed pores. Also, it is quite likely that at these temperatures superheated steam is

Table I

Average Degrees of Super-Contraction Associated with Fiber Elongation for Sets of Five Fibers Subjected to Three Hot-Iron Treatments at a Temperature of 180°C with a Hot-Iron Speed of 1.0 in/s

Fiber no.	% Extension	% Super-contraction
1	15.7	3.1
2	13.2	2.6
3	12.4	2.8
4	11.2	2.4
5	10.7	2.7
6	10.3	3.1
7	9.8	2.5
8	9.5	1.7
9	8.7	2.3
10	8.4	1.9

The hair fibers showed pore formation immediately after hot-iron treatment. Super-contraction was produced in these fibers after they were wet for 3 min and then heated again at 150°C .

involved, both, in the process of protein denaturation and hair straightening. Superheated steam is steam at a temperature higher than water's boiling point and it is quite possible that the hair moisture inside the cortex rapidly vaporizes and superheats when the hot iron temperature is higher than 150°C.

EFFECTS OF TEMPERATURES HIGHER THAN 180°C AND LOW HOT-IRON SPEEDS

Thus far the effects of temperatures ≤ 180 C and normal hot iron speeds (~ 1 in/s) on pore formation have been analyzed. In the following sections the effects of hot iron temperatures in the range of $180 > 210^\circ\text{C}$ but with lower speeds (~ 0.2 inch/s) will be analyzed. When the hot-iron speeds were reduced to ~ 0.2 inch/s and the temperature was kept at 180°C a few pores started to appear deeper inside the cortex. These deeper pores were observed to coexist with a few voids of larger size (see Figure 10). Further increases in temperature to $\sim 210^\circ\text{C}$ while still maintaining low hot iron speeds, resulted in the appearance of larger voids approximately 3 to 10 μm inside the cortex. For instance, Figure 11a shows the image of a hair fiber hot ironed at 210°C and obtained without shift in plane of focus. The level of cuticle sheath integrity observed in this image indicates again that, when the microscope's plane of focus is at the hair surface, no apparent damage in the fiber is detected. However, when the microscope's plane of focus is shifted to regions inside the cortex, the presence of large voids becomes apparent (see Figures 11b and 11c).

Further increases in the hot iron temperature to $\sim 220^\circ\text{C}$ and above with low speeds resulted in the formation of air bubbles approximately 20 to 30 μm in size. The appearance of these air bubbles inside the cortex could easily be detected by optical microscopy as they produced bright large spots due to their diffuse pattern of light scattering. Furthermore, the appearance of these air bubbles was invariably accompanied by severe fiber shape deformation (see Figures 12a, 12b, 12c, and 12d) and by a brittle transformation of the whole hair fiber. After this process the fiber broke into small fragments with a minimum force. This type of protein transformation in the hair fibers constitutes the most severe

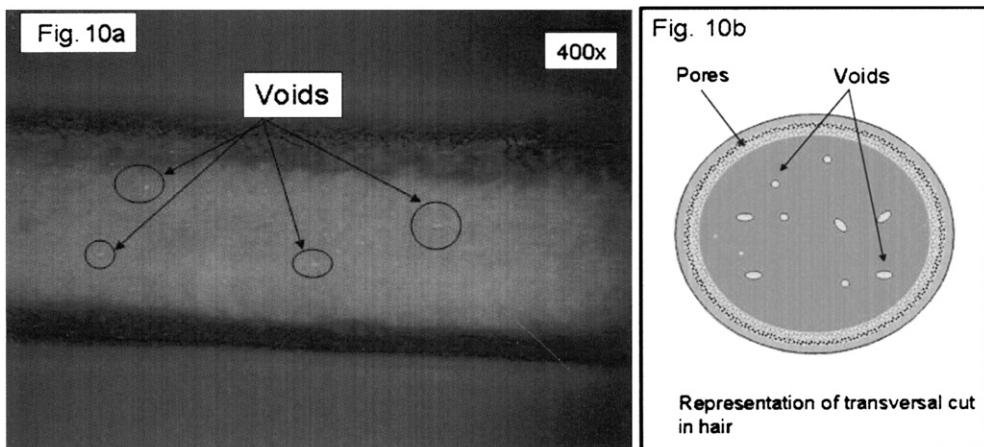


Figure 10. Micrograph of a hair fiber ($\phi \sim 72 \mu\text{m}$) showing the formation of larger voids (inside circles) deeper inside the cortex at a distance of $\sim 24 \mu\text{m}$ from the hair surface. The fiber was subjected to five hot-iron treatments at 180°C using a hot-iron speed of ~ 1 in/s.

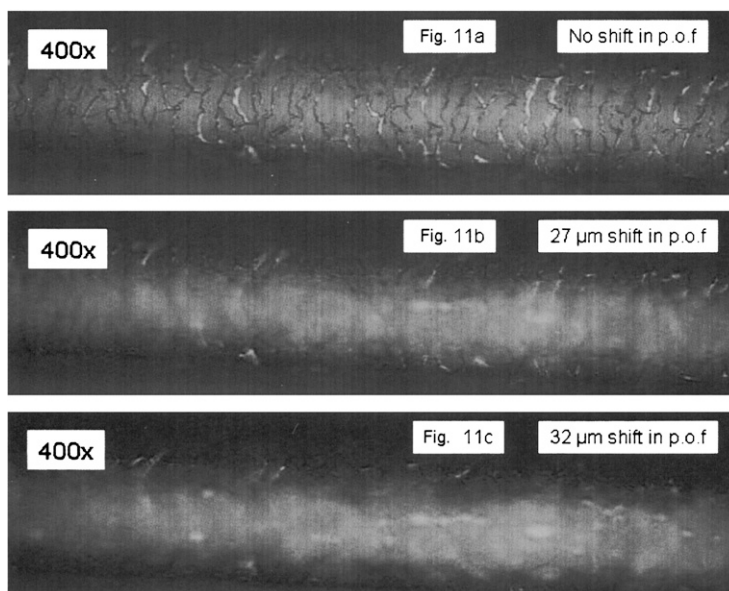


Figure 11. Micrograph of a hair fiber ($\phi \sim 64 \mu\text{m}$) showing image of surface obtained with no shift in plane of focus (11a). Later the plane of focus (p.o.f.) was shifted in 27 and 32 μm , respectively; the white spots in the image are voids with sizes ranging between 3 and 10 μm . The hair fiber was subjected to five hot-iron treatments at a temperature of 210°C and with a hot-iron speed of 0.2 in/s.

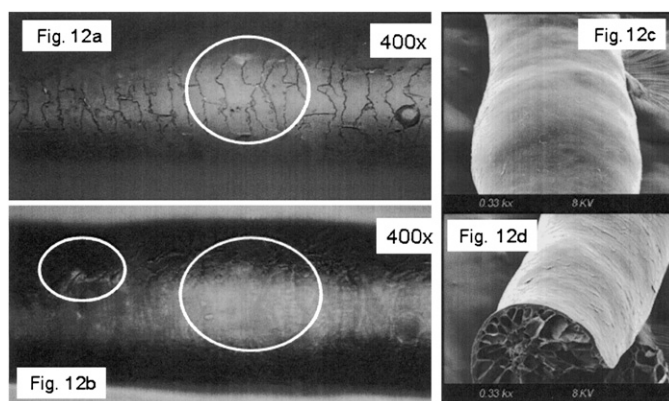


Figure 12. Micrograph of a hair fiber ($\phi \sim 78 \mu\text{m}$) before (12a) after (12b) shifting the plane of focus. Figure 12b shows the formation of small voids and air bubbles inside the hair after being subjected to one hot ironing treatment at 220°C with a hot-iron speed of 0.2 in/s. The air bubbles appear as luminous translucent regions by optical microscopy. In Figures 12c and 12d are shown different views of the same fiber when seen by scanning electron microscopy.

form of heat damage. It certainly, involves a process of protein denaturation, melting, aggregation, and shrinkage similar to the one taking place when other types of proteins are exposed to high temperatures during cooking (15). It is interesting to note also that SEM analysis of the broken fragments showed that large air bubbles and micro-pores always coexist together (see Figures 13a and 13b).

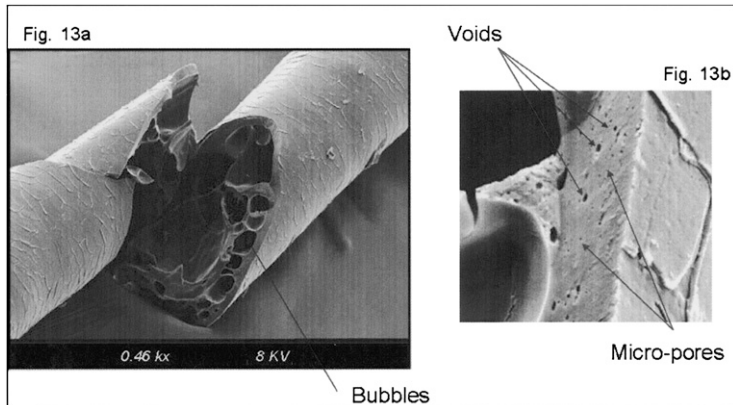


Figure 13. Scanning electron micrograph of a hair fiber ($\phi \sim 68 \mu\text{m}$) after being subjected to four hot-iron treatments at 220°C using a low hot-iron speed of ~ 0.2 in/s.

EFFECTS OF SOME POLYMERS AND OILS ON THE HAIR SURFACE

It should be mentioned here that the application of polymers and oils on the hair surface prior to hot iron application had a significant impact on the heat damage of both cuticle sheath and cortex. For instance, the experiments showed that for temperatures $< 180^\circ\text{C}$ and normal hot iron speeds, the presence of thick polymer layers on the hair surface led to the formation of pores that were mostly confined at the cuticle sheath surface, while the number of pores inside the cortex decreased substantially. This effect can be seen in Figure 14 where it is shown that when a thin polymer layer ($\sim 0.5 \mu\text{m}$ thick) of N-vinylpyrrolidone methacrylamide and N-vinyl imidazole (16) is on the hair surface the number of pores formed inside the cortex is lesser than when the polymer is absent. Also, it was observed that this polymer suppressed the formation of the type of large voids occurring at 210°C

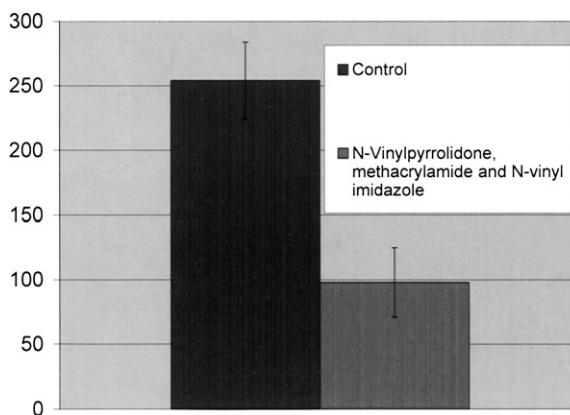


Figure 14. Averages of total pore count from areas $\sim 0.06 \text{ mm}^2$ for two sets of ten hair fibers ($\phi \sim 72 \mu\text{m}$). The bars represent average counts obtained with untreated fibers (control) and fibers treated with a leave-on formulation containing 0.1% aqueous solution of N-vinylpyrrolidone methacrylamide and N-vinyl imidazole (13); after application the excess solution was squeezed with the fingers. All hair fibers were subjected to five hot-iron treatments.

with low hot-iron speeds. Instead the polymer shifted their formation temperatures to levels higher than 220°C.

In summary, the above described experiments suggest that the following mechanism is responsible for heat damage to the cortex in hair fibers subjected to hot irons. When a hot iron is in contact with hair heat transfer takes place. This heat transfer creates a temperature gradient inside a hair fiber from the cuticle sheath to the center of the cortex. The profile of this temperature gradient is dependent on the contact time of the hot iron with the hair fiber. If the hot-iron speed is fast or normal the gradient will be steep, and only regions at the periphery of the hair cortex will get affected by heat flow and high temperatures. Thus, protein denaturation and explosive water evaporation will occur mainly at the cortex periphery leading to the production of micropores in these regions such as observed with normal hot iron speeds and temperatures $\leq 180^\circ\text{C}$ (see Figures 2 and 7).

In contrast, when the hot-iron speeds are reduced, a larger contact time between hot-iron and hair surface is established. This will allow for a higher heat transfer and ultimately will lead to higher temperatures inside the hair fiber causing, thereby, an incipient process of protein melting and shrinkage. Consequently, low hot iron speeds and temperatures between $180^\circ\text{C} < T \leq 210^\circ\text{C}$ will produce larger voids deeper inside the cortex (see Figs. 10 and 11). For hot iron temperatures higher than 220°C at low speeds more heat flow will take place. This process will generate high temperatures inside the hair with values very close to those at the hot-iron surface. These high temperatures will create, thus, the massive process of protein melting, shrinking, and aggregation with the consequent production of large bubbles, hair shape distortion, and fiber fragmentation as depicted in Figs. 12 to 13.

Finally, the effect of polymer layers on the formation of micropores can be explained by considering that, when a polymer material is deposited on the hair surface, it acts as a thermal buffer that slows heat transfer and reduces the explosive water evaporation that occurs in regions deep inside the cortex. It is worth mentioning here, that the presence of thin layers of polymers on the hair surface also modified the patterns of friction damage at the cuticle sheath. The topic of friction damage by hot-irons is presently being studied and will be the subject of another report.

CONCLUSIONS

Heat damage by hot irons was found to be dependent on the heat transfer to hair and to be determined by the conditions of temperature and hot-iron speed. The various types of damage appearing in the hair cortex in the form of micropores, large voids, and air bubbles were found to involve protein changes ranging from protein denaturation, melting, aggregation, and shrinkage depending on the temperature. Water evaporation and mechanical extension were shown to play a critical role in the degree of micropore formation. With normal hot-iron speeds and temperatures not higher than 200 °C most of the damage in the form of pores was confined to the cortex periphery and to the cuticle sheath. With higher temperatures and lower speeds damage was extended to regions deeper inside the cortex. The presence of polymer layers on the hair surface appears to shift micropore production from the cortex to the cuticle sheath and also, to increase the resistance for the formation of larger voids.

REFERENCES

- (1) P. Milczarek, M. Zielinski, and M. L. Garcia, The mechanism and stability of thermal transition in hair keratin, *Colloid Polym. Sci.*, **270**(11), 1106–1115.
- (2) J. Cao and F. Leroy, Depression of the melting temperature by moisture of the α -form crystallites in human hair keratin, *Biopolymers*, **77**(1), 38–43 (2005).
- (3) F. J. Wortmann, G. Sendelbach, and C. Popescu, Fundamental DSC investigations of α -keratinous materials as basis for the interpretation of specific effects of chemical, cosmetic treatments on human hair, *J. Cosmet. Sci.*, **58**(4), 311–317 (2007).
- (4) D. Istrate, C. Popescu, and M. Moller, Non-isothermal kinetics of hard alpha-keratin thermal denaturation, *Macromol. Biosci.* **9**(8), 805–812 (2009).
- (5) R. McMullen and J. Jachowicz, Thermal degradation of hair. I. Effect of curling irons, *J. Cosmet. Sci.*, **49**, 223–244 (1998).
- (6) Y. Zhou *et al.* Investigation of thermal damage of hair from hot flat ironing and the thermal protective effects of cosmetic pretreatments, *Proceedings of the 26th IFSCC Congress, Argentina, September 20–23, 2010*.
- (7) S. B. Ruetsch and Y. K. Kamath, Effect of thermal treatment with a curling iron on hair fiber, *J. Cosmet. Sci.*, **55**, 13–27 (1998).
- (8) R. L. McMullen and S. P. Kelty, Investigation of human hair fibers using lateral force microscopy, *Scanning*, **23**(5), 337–345 (2001).
- (9) C. Scanavez, M. Silveira, and I. Joekes, Human hair: Color changes caused by daily care damages on ultra-structure, *Colloids Surf. B*, **28**(1), 39–52 (2003).
- (10) M. Schaffer, V. Hill, and T. Cairns, Hair analysis for cocaine: The requirement for effective wash procedures and effects of drug concentration and hair porosity in contamination and decontamination, *J. Anal. Toxicol.*, **29**(5), 319–326 (2005).
- (11) M. Feughelman, *Mechanical Properties and Structure of Alpha-Keratin Fibres; Wool, Human Hair, and Related Fibers* (University of New South Wales Press, 1997).
- (12) S. Ogawa, K. Fujii, K. Kaneyama, K. Arai, and K. Joko, A curing method for permanent hair straightening using thioglycolic and di-thioglycolic acids, *J. Cosmet. Sci.*, **51**, 379–399 (2000).
- (13) L. J. Wolfram and M. K. Lindemann, Some observations in the hair cuticle, *J. Soc. Cosmet. Chem.*, **22**, 839–850 (1971).
- (14) J. Cao and A. Y. Bhojro, Structural characterization of wool by thermal mechanical analysis of yarns, *Textile Res. J.*, **71**(1), 63–66 (2001).
- (15) T. R. Dutton and M. W. Orcutt, Chemical changes in proteins produced by thermal processing, *J. Chem. Educ.*, **61**(4), 203 (1984).
- (16) N-vinylpyrrolidone methacrylamide and N-vinyl imidazole; BASF polymer Luviset Clear.